Simulation-Driven Design of Restrained Pipe Joints

Guido M. Quesada

Professor, School of Mechanical Engineering, University of Costa Rica, San José, Costa Rica

R&D Advisor, Mechanical Problem Solving S.A., 314 Oficentro Centauro, Esquivel Calle Blancos, Costa Rica

Abstract: This paper shows how multiple analysis techniques converge in Abaqus/Standard to produce simulation-driven design of restrained PVC pipe joints. PVC is known to exhibit viscoelastic behavior as it approaches its glassy transition temperature. This is used to produce pipe sockets by heating and forming them over a mandrel. A type of pipe joint which is becoming very successful includes other elements such as special seals made or rubber and steel, and restraint mechanisms made of ductile iron, which remain trapped inside the socket when it cools. At room temperature, elastic-plastic behavior of PVC dominates. As the restraint mechanism grips a spigot inserted in the socket, the pipe is indented by sharp teeth, causing severe plastic strain and mesh distortion. This makes a good case for an Adaptive Langragian-Eulerian domain. Since viscoelastic and elastic-plastic material models are incompatible, the results of the socket-forming model are transferred into the joint assembly and test model, in which some of the parts are put back together using automatic interference fit. Furthermore, there is hyperelastic behavior in the seal, with large deformation, as well as some plastic strain in the steel and ductile iron components. All this happens in a rather tight space, with multiple contact interactions, sliding with friction, fluid pressure, axial thrust and in some cases bending of the joint. Besides proving an excellent design tool, Abaqus/Standard provided an interesting showcase of several nonlinear FEA techniques that can be put together in a model.

Keywords: Assembly Deformation, Bending, Design Optimization, Elasticity, Experimental Verification, Forming, Hyperelasticity, Interface Friction, Mechanisms, Pipes, Plasticity,Residual Stress, Rubber, Rubber Seals, Seal, Shrink Fit, Viscoelasticity.

1. Introduction

Bell-and-spigot gasket-joint thermoplastic pipes such as Polyvinyl Chloride (PVC) are widely used in pressure applications for potable water distribution and transmission, and sewer force mains. One of the most common types of joints is a push-on joint with a "locked-in" gasket, commonly referred to as the Rieber joint. To produce this type of joint the gasket is placed on a steel mandrel which has the required shape to form the bell. The pipe is then heated until it softens, pushed into the mandrel, over the seal, and allowed to cool down. Once the formed shape is fixed, the socket is pushed out by an auxiliary collar and allowed to continue cooling to room temperature, with the Rieber gasket "locked-in". This process is known as belling. The Rieber gasket is reinforced with an adjoining external or internal steel ring or band, so it can withstand the loads applied during belling. This reinforcement also provides structural support and pre-compression of the rubber ring against the pipe.

The thrust forces which result at joints due to changes in the direction or in the diameter size of a pipeline under pressure must be counterbalanced to prevent joint separation. This is accomplished using concrete thrust blocks or joint restraint devices. Restraint mechanisms internal to the bell of the pipe or fitting were first developed for iron pipe in Germany by Duker over 20 years ago. U.S. Pipe (an iron pipe manufacturer) introduced a restrained gasketed system to the US pipe market in the mid-1980s. Recently, a similar system has been developed for PVC under the brand name of Bulldog™ (Quesada, 2005). This joint restraint system is integral to the bell of a PVC pressure pipe or fabricated fitting and is incorporated into the product during manufacture.

The current version of the Bulldog™ restrained pipe joint is designed for integration into AWWA C900 PVC pipe and fittings in diameters 4-inch through 12-inch (larger sizes are currently under development). The mechanism consists of a metal casing that sits adjacent to the Rieber gasket in the bell. The casing and the seal are molded into the raceway of the bell during pipe belling. A C-shaped grip-ring with several rows of uni-directional serrations is manually inserted into the casing after the belling process. Both the casing and the grip ring are made of ductile iron that has been coated using an electro-coating process that achieves a uniform thickness and provides corrosion resistance. Figure 1 shows a cross-cut view of the components in the joint (Fisher, 2009).

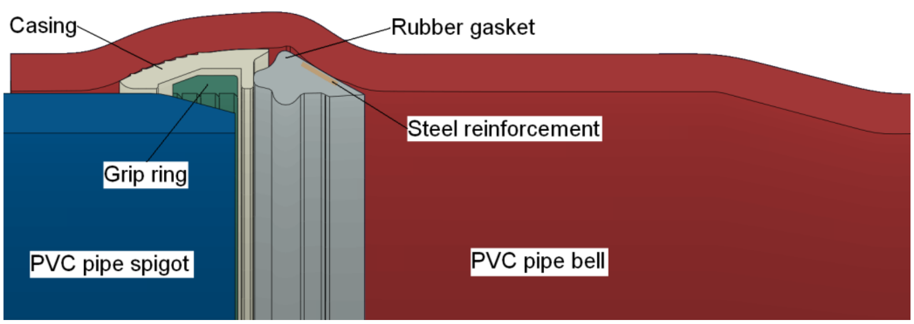

Figure 1. Cut out view of a restrained pipe joint model

When the pipe arrives at a jobsite, the bell already contains the seal and the casing with the grip ring inserted in it. The joint is assembled like a regular push-on joint: The spigot is pushed into the bell up to an insertion mark. Figure 2 shows an assembled joint and a manual pipe-puller that makes assembly easier (Fisher, 2009).

Another application of this type of joint is pipe installation by Horizontal Directional Drilling (HDD). In this application, instead of digging a trench for the pipe, a tunnel is drilled, leaving a cable inside. This cable is attached to a puller device which grips the pipe and pulls it along the tunnel. In this case a chain of pipe assemblies must be pulled, applying considerable force to the joint restraints. Furthermore, because the tunnel starts and ends at an angle with respect to the ground, the joint must be able to sustain a significant degree of bending (Fisher, 2009, Najafi, 2009).

Figure 2. Typical field installation of a restrained pipe joint.

FEA simulation of all these aspects of the restrained pipe joint forming and loading is very useful for making decisions about its performance and structural optimization.

2. Material properties

2.1 Rigid surfaces for belling equipment

The belling mandrel and its accessories, such as a "loader" device to put the seal in position and an auxiliary collar to push out the bell after belling (sometimes excluded from the model for simplicity), are modeled as rigid surfaces. They are truly rigid compared to other components and there is no interest in their state of stress within the scope of the project described in this paper.

2.2 Elastic-plastic model for steel

The steel reinforcement in the seal is modeled as a simplified piecewise linear elastic-plastic material. There is actually a chance for this reinforcement to undergo some plastic deformation, during the belling process. For AISI 1010, a rather weak low-cost steel, the modulus of elasticity would be 207GPa, the Poisson's modulus is 0.29, yield strength is 180 MPa, and ultimate stress is 320 MPa at 0.28 strain.

2.3 Elastic-plastic and orthotropic models for grip and casing ductile iron

Ductile iron in the casing and the grip ring is modeled as a simplified piecewise linear elastic-plastic material. There may be little plastic deformation in the gripping ring, though generally negligible. For DI 70-50-05, the modulus of elasticity would be 165GPa, the Poisson's modulus is 0.29, yield strength is 345 MPa, and ultimate stress is 485 MPa at 0.05 strain.

Since the simulation driven design process is iterative and computational resources are limited, a fast 2D axisymmetric model is highly desirable. However, the griping ring is not axisymmetric, it is a “C”. Therefore it has a discontinuity in its circumference. As a result, the grip appears to have a much lower stiffness in the hoops direction than in the axial or radial direction. This is addressed by actually giving special orthotropic properties to the grip ring. First a true 3D model of the ring is created and deformed as it would in operation, then a 2D model is used to calibrate the orthotropic constants and obtain an equivalent behavior. The result will change depending on grip ring size and shape.

2.4 Elastic-plastic model for PVC

PVC requires two separate models, since they are mutually exclusive. The first one is a simple piecewise linear elastic-plastic model. Material properties are taken for PVC cell class 12454 as defined by ASTM D1784 (Unibell, 2001), according to AWWA C900 Standard. The modulus of elasticity is 2758 MPa, the Poisson’s modulus is 0.38, yield strength is 48.3 MPa, and ultimate stress is defined conveniently to allow some plastic deformation without making the model unstable.

2.5 Viscoelastic model for PVC

Viscoelastic modeling of PVC deserves special consideration since the conclusion that this was the adequate model for the belling process was not obvious. As a polymer, PVC is an amorphous material, which doesn’t have a melting temperature. Instead, its mechanical properties undergo a gradual transition from a solid behavior into a liquid behavior. The middle point in this transition is called the glassy transition temperature T_g. For PVC, the glass transition temperature is around 90°C. At room temperature PVC is far below its glass transition, therefore it behaves very much like an elastic-plastic solid. PVC does undergo creep and stress relaxation at room temperature (which is a viscoelastic behavior), but these take thousands of hours and can be neglected for practical purposes.

As PVC approaches the glass transition, it starts behaving more like rubber, with a much lower modulus of elasticity, tolerance to large deformation, good elastic recovery and relatively fast relaxation. Past the glassy transition, it becomes a supercooled fluid, which still has an instantaneous or apparent elasticity but is able to relax or flow indefinitely. As temperature keeps increasing the elastic behavior vanishes and the material behaves completely like a viscous fluid.

For the purpose of belling, the PVC is heated slightly below the glass transition temperature. At this temperature, it can be manipulated as a solid and also deformed into the shape of the bell. When the material is cooled down, the viscosity and the elastic modulus recover their original room temperature values. If the deformation is held while the material is cooled, the shape acquired will be frozen by the effect of a very large viscosity, into the mainly solid elastic behavior that PVC exhibits at room temperature.

It is worth noting that during this process, the amount of plastic or permanent deformation is negligible. If the pipe is heated again, the viscosity will decrease again, releasing nearly the original shape of the pipe. This is known as “memory” of the PVC. In order to model this behavior, it is necessary to use a viscoelastic model (Quesada, 2000). This model combines the initial elastic behavior, with a relatively high modulus of elasticity E_0, and a viscous behavior that enables a relaxation over time to a much lower elastic modulus E_∞.

The effect of temperature is a reduction of the modulus of elasticity, but also a shift in the logarithmic time scale. This means that at higher temperatures the curve will shift to the left so the relaxation occurs faster, and vice versa. Notice that this behavior is verified only near the glass transition temperature. At room temperature the viscous behavior vanishes and PVC is better modeled as a linear-elastic solid (unless long term effects are studied), while at injection temperatures the elastic behavior vanishes and the PVC is better modeled as a viscous fluid.

The isotropic linear elastic model (Lakes, 1998) is sufficient for the purpose of belling PVC pipe. Anisotropic modeling would become necessary only if there is a significant alignment of the polymer strands in a particular direction (for example in pipes that are extruded at a small diameter and then expanded to their final diameter). After splitting strain into deviatoric and volumetric, the linear isotropic viscoelastic model can be expressed as follows:

$$\boldsymbol{\sigma}(t) = \int_0^t 2G(\tau - \tau')\frac{d\mathbf{e}}{dt'}dt' + \mathbf{I}\int_{\mathbf{0}}^{\mathbf{t}} K(\tau - \tau')\frac{\mathrm{d}\phi}{dt'}dt'$$

where $\boldsymbol{\sigma}$ stress, t is time, G is the shear modulus, τ is the reduced time (by effect of temperature), τ' is the reduced time evaluated at an integration time variable t', $\mathbf{e}$ is deviatoric strain, **I** is the identity matrix, K is the volumetric modulus and ϕ is volumetric strain. This splitting is important because the viscoelastic effect is mostly deviatoric, while bulk modulus remains nearly constant. The reduced time τ is calculated as follows with the aid of a time shift function:

$$\tau = \int_0^t \frac{dt'}{A_\theta\big(\theta(t')\big)}$$

where θ is temperature and A_θ is a time shift function. The shift function used is the Williams-Landel-Ferry (WLF) equation, which has the following form:

$$-\log(A_\theta) = \frac{C_1(\theta - \theta_0)}{C_2 + (\theta - \theta_0)}$$

Where θ_0 is a reference temperature, typically the glass transition temperature, and C_1 and C_2 are constants, which seem to vary only slightly from polymer to polymer. Typical reference values are 17.44 and 51.6. Notice that as the temperature θ approaches $\theta_0 - C_2$, the time shift function tends to 0, and the effective relaxation time tends to infinity. Below this temperature, the WLF equation is invalid. In order to deal with this singularity, for $\theta \leq \theta_0 - C_2$,, Abaqus drops the viscoleastic behavior and the model becomes fully elastic. A thermal expansion coefficient of 5.4E-05/°C is used in order to account for thermal contraction of the bell as it cools down in this fully elastic state.

The relaxation functions for the elastic moduli are based on a normalized series of exponentials known as the Prony series:

$$G(t) = G_0\left(g_\infty + \sum_{i=1}^{n} g_i e^{-t/\tau_i}\right)$$

$$K(t) = K_0\left(k_\infty + \sum_{i=1}^{n} k_i e^{-t/\tau_i}\right)$$

Where g_i and k_i are the relative moduli of terms *i*. Note that $g_\infty=1-\sum g_i$ and $k_\infty=1-\sum k_i$, therefore g_∞ and k_∞ are not required as input data. τ_i are the relaxation times of terms *i* and n is the number of terms used. For practical purposes a single Prony coefficient is sufficient, since intermediate states are not of interest. Also because the greatest relaxation occurs in deviatoric strain while the material remains incompressible, g_1 will be close to 1 while k_1 will be close to 0.

The temperature chosen for the belling process is taken from manufacturing practice and adjusted in the model as necessary to obtain the desired results, very much the same way it is done in real life.

2.6 Hyperelastic model for rubber

For the rubber in the seal, it is found that a hyperelastic Marlow model from uniaxial tension data is sufficient. Figure 3 shows typical stress-strain curves for this material.

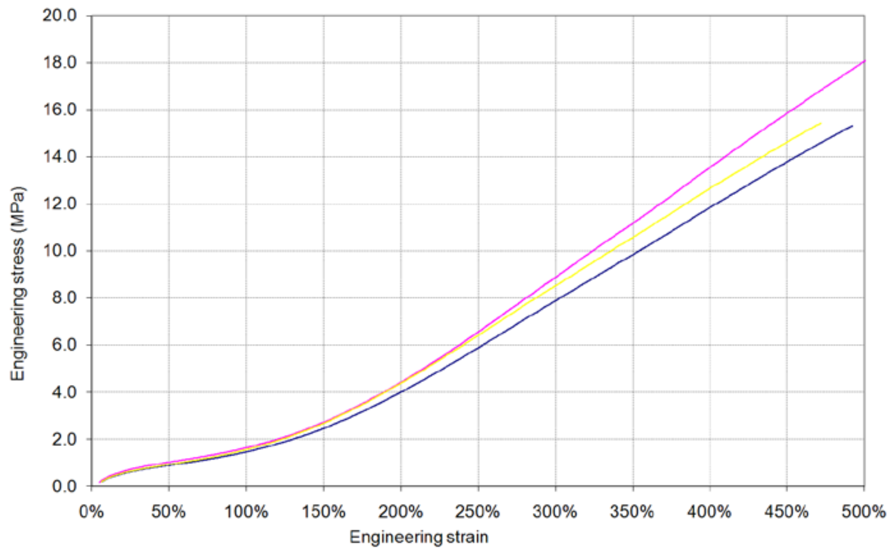

Figure 3. Stress-strain curve for uniaxial tension test of rubber

3. Simulation of the pipe belling process

The belling model proceeds in several steps. First the casing and the seal are loaded on the mandrel. This can be done by pushing them axially over an assembly ramp or by allowing Abaqus to resolve the interference fit into the loaded position. Figure 4 shows the solution of the interference fit, which runs much faster than the axial assembly and renders acceptable results (friction coefficients may cause slight differences). In the meantime the socket is heated in order to reach a softened viscoelastic state. Then it can also be pushed over the mandrel or expanded before activating contact interactions and allowed to rest on the assembly. The latter approach also runs faster.

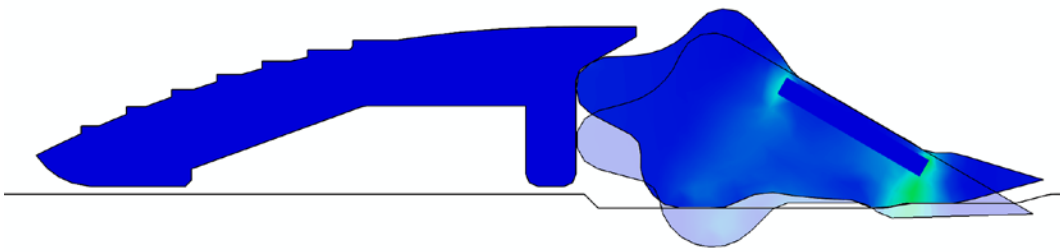

Figure 4. Loading of casing and seal on the mandrel by automatic interference fit.

Figure 5 shows a region of interest of the softened socket, the casing and the seal mounted on the belling mandrel. The stress scale is chosen with respect to the PVC yield strength. As one might expect, the general state of stress is low, since the PVC is softened. Only the steel band reinforcing the seal shows significant stress, mostly because it is pressing the seal tail against the mandrel.

Notice how the softened socket copies relatively small details such as the seal's apex and the serrations around the casing. At this step some vacuum or external pressure is applied in order to aid the forming process.

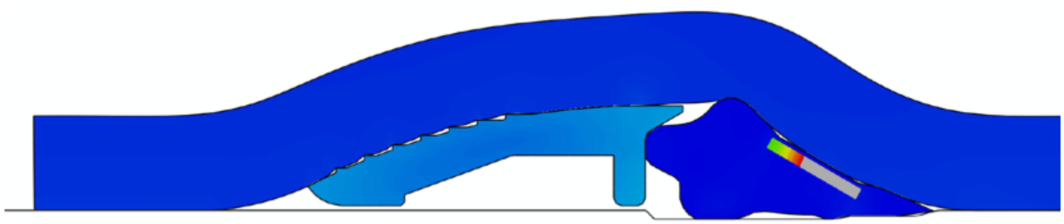

Figure 5. The belling process before cooling the socket

Once the socket is allowed to cool down and removed from the belling mandrel, it becomes fully elastic and it undergoes thermal contraction. Due to this, it develops residual stress against the casing. This in turn helps keep the casing firmly fixed to the socket. This is shown in figure 6.

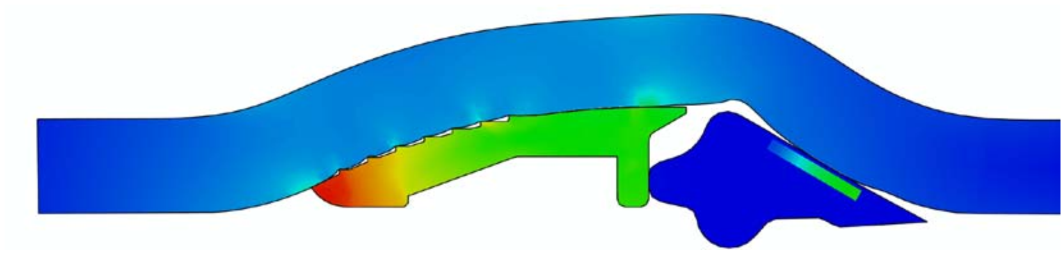

Figure 6. The restrained joint socket after removal from the belling mandrel

4. Simulation of joint assembly and pullout in straight alignment

For most cases in 2D axisymmetric models, assembly and testing of the joint in straight alignment proceed as additional steps after the belling simulation. Restarting the analysis or simulating the test from imported belling results can be advantageous in order to save time if there is need to rerun the tests. However if there are design changes these affect the belling as well. Also there are two different types of tests: one is the hydrostatic test, in which fluid pressure is applied and enabled to produce a resulting axial thrust which would try to separate the joint; the other one is axial pulling in straight alignment without fluid pressure for the purpose of HDD (Fisher 2009), which is shown as illustration for this paper. Figure 7 shows the model as the spigot is moving into the socket. At this point the grip has been installed and is floating inside the casing.

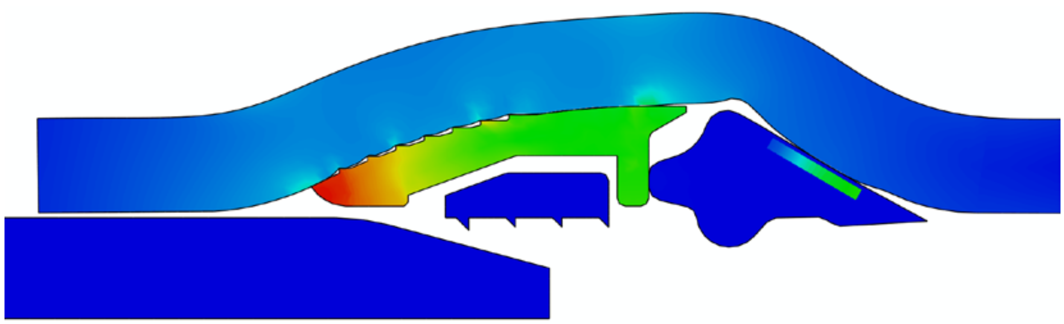

Figure 7. Pipe joint at the beginning of the assembly

Figure 8 shows the joint after assembly is completed. The spigot has opened the grip ring and pushed it towards the bottom of the groove in the casing. Also the seal is compressed between the spigot and the socket.

Figure 8. Pipe joint after assembly

Figure 9 shows a detail of mesh refinements used. It also shows a spring which is used to provide rotational stiffness to the grip ring, since this stiffness is lost due to the orthotropic material model. Notice there is a preconditioned mesh on the spigot under the grip teeth. This mesh region also defines an adaptive Lagrangian-Eulerian domain (ALE), which helps overcome mesh distortion as the grip sinks its teeth into the pipe. This is actually a rather rough model, but it is sufficient for the structural evaluation of the assembly. Finer meshes have been used in other models to evaluate and improve tooth shape.

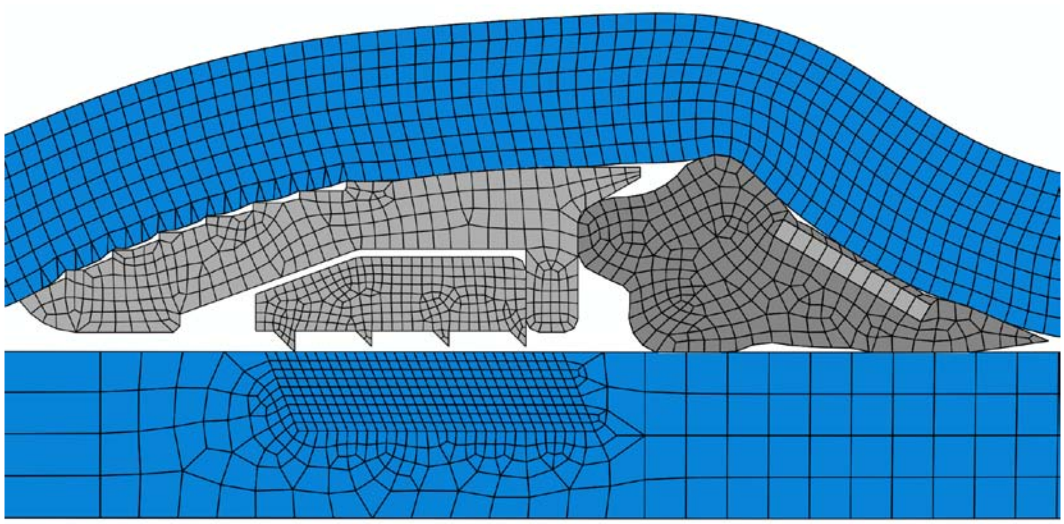

Figure 9. Mesh details

After inserting the spigot, it is pulled back using a prescribed displacement until it the analysis job aborts. Alternatively internal fluid pressure would be applied (up to a standard prescribed test pressure). As the spigot is pulled, it drags the grip ring with it. Thanks to a favorable combination of friction coefficients the grip slides along its mating conical surface on the casing and closes, thereby sinking its teeth into the spigot. A grip stop is provided in order to avoid excessive gripping load, which could generate excessive stress both on the spigot and the casing. Figure 10 shows the axial pull at an advanced state. At this point yield stress is exceeded at several locations on the spigot and the socket, which are then very likely to fail. This helps identifying the weakest points in the joint and trying out design changes that will in turn help improve the design.

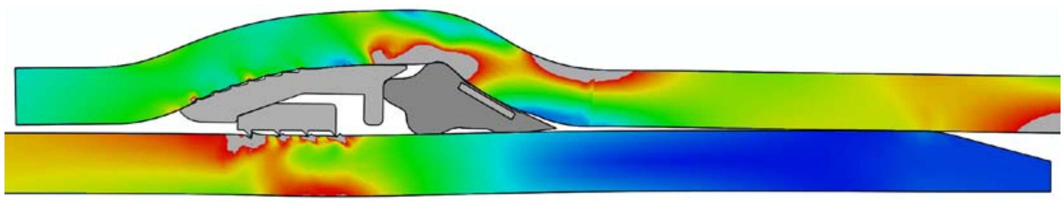

Figure 10. Axial pull in straight alignment

As a matter of fact, the joint restraint design has improved so much that in destructive laboratory tests the pipe often fails away from the joint. Several stages during the pull out test are identified in order to evaluate how the restraint engages and performs before it is taken to failure. Figure 11is a typical force-displacement plot showing these stages, which is in agreement with physical testing (Najafi, 2009).

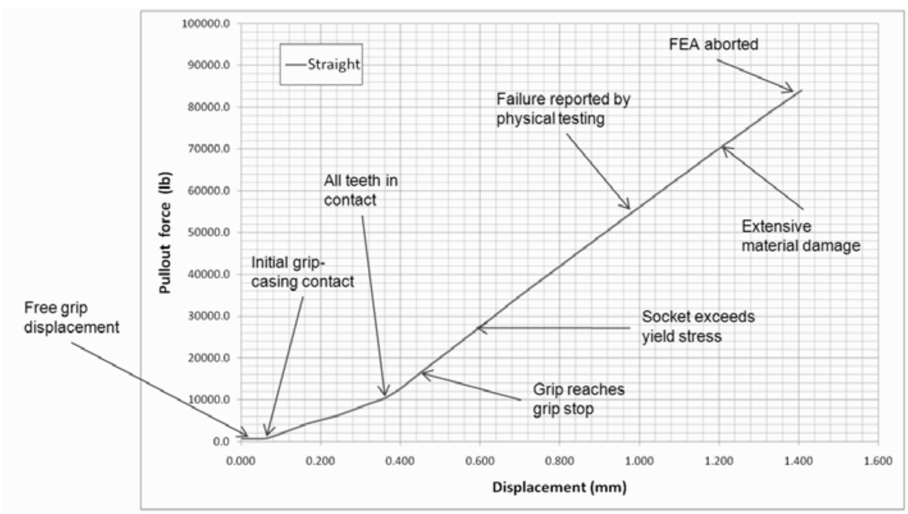

Figure 11. Axial pull force-displacement plot

5. Simulation of assembly and pullout with bending

Pullout with bending requires a 3D model. However, the 2D socket geometry created from the belling simulation is turned into a sketch and used to generate a 3D solid, so a 3D belling simulation is not necessary. This approach gives better control over the 3D meshing process. This socket is put together with the casing by automatic interference fit, producing a similar state of stress as in the 2D model. Next the spigot insertion is performed in straight alignment, in a similar fashion as the 2D model. For simplicity the seal is excluded in this particular job.

After inserting the spigot into the socket, the assembly is held by the free ends of the two pieces of pipe and subjected to a lateral displacement, in order produce a state of fairly pure bending at the joint. Figure 12 shows the state of stress at the joint. Notice how the stress flows from the tip of the spigot to the edge of the socket mouth. It is also important to notice that in this condition the grip is no longer aligned to the spigot, therefore grip engagement will not be uniform.

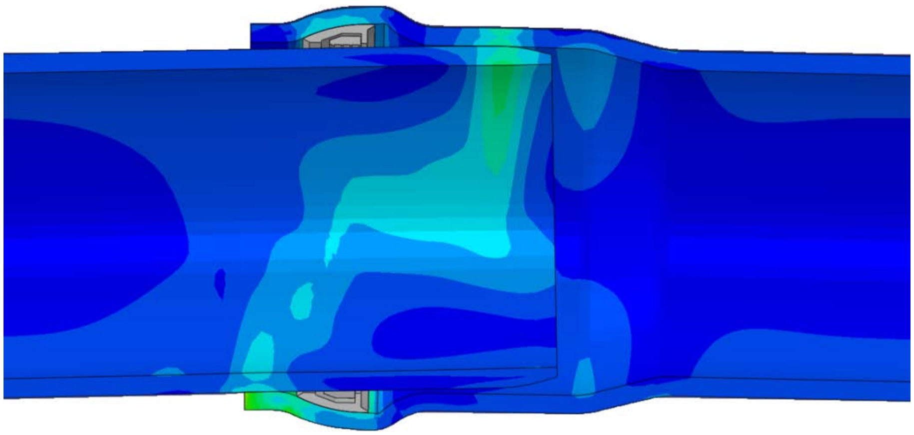

Figure 12. Bending of the assembly

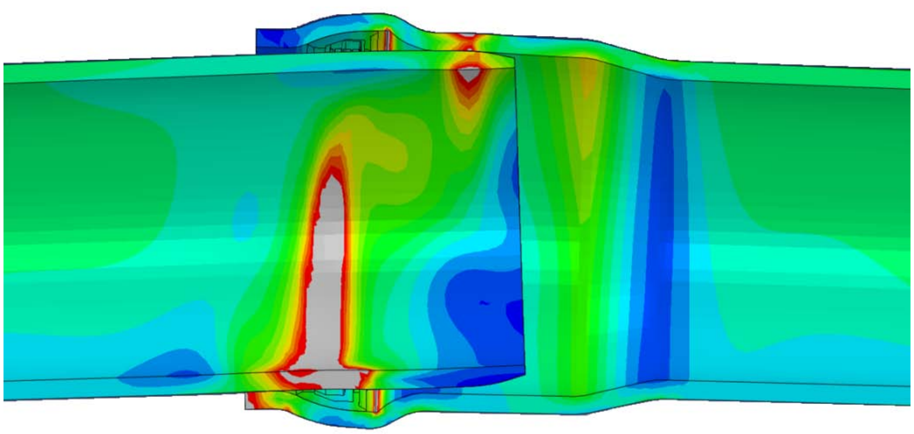

Figure 13. Bending and pulling of the assembly

Finally the assembly is pulled apart while holding the state of bending. Figure 13 shows the model near the point when the Abaqus job aborts. At this point the pipe is already severely damaged (yield strength exceeded). Uneven engagement of the grip on the spigot concentrates stress on about half the surface that would have engaged in straight alignment. This causes the joint to fail much earlier, as shown in figure 14. Further analysis shows that this problem can be reduced by pulling the joint in straight alignment before applying bending, at least enough to ensure uniform grip engagement. This is actually how it is currently done in the field and the test laboratory.

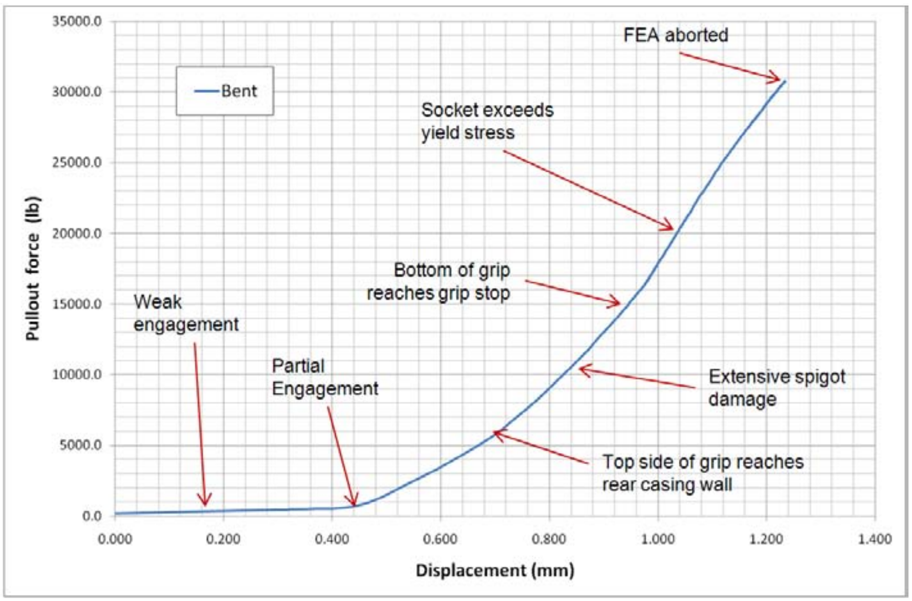

Figure 14. Force-displacement plot for axial pull in bending

6. Conclusion

A family of high performance restrained pipe joints for PVC have been produced for sizes from 4" to 12" and are currently being extended to larger sizes. This development would have been impossible without nonlinear FEA simulation, as it has provided accurate information about joint performance and the weak spots that require changes in design. Furthermore FEA has provided useful information about the best way to apply this joint in the field and about the way it should be tested in the laboratory.

This particular development project was also a good opportunity to put a range of Abaqus/Standard functionalities together into a fast iterative analysis and design process with very affordable computational resources.

7. References

1. Fisher, Craig, and Quesada, Guido, “Tensile Testing of a Push-On Restrained Joint PVC Pipe,” Technical Report, S&B Technical Products, Fort Worth, Texas, USA, 2009.
2. Lakes, Roderick S., “Viscoelastic Solids”, First Edition, CRC Press, New York, USA,1998.
3. Najafi, Mohammad, and Ramírez, Guillermo, “Testing of Bulldog PVC Restraint Joint for Trenchless Technology,” University of Texas at Arlington, Arlington, Texas, USA, 2009
4. Quesada, Guido, “Viscoelastic Modeling of PVC for Belling Analysis,” Technical Report, TERRAMIX, San José, Costa Rica, 2000.
5. Quesada, Guido, “Characterization of a Successful Prototype for 12” Rieber Self Restrained Joint”, Report HT0511r01, Mechanical Problem Solving, San José, Costa Rica, 2005.
6. Quesada, Guido, “Bulldog Restraint System C900 8” Performance Analysis for Horizontal Directional Drilling,” Report HT091101, Mechanical Problem Solving, San José, Costa Rica, 2009.
7. Rahman, Shah, and Bird, Wayne, “PVC Pipe Jointing: The Rieber System in North America, Technical Report, S&B Technical Products Literature, Fort Worth, Texas, USA, 2006.
8. Uni-Bell PVC Pipe Association, “Handbook of PVC Pipe: Design and Construction,” 4th Edition, 2001, Dallas, Texas, USA.